Supplementary Material

Neuroprotective Potential of a Small Molecule RET Agonist in Cultured Dopamine Neurons and Hermiparkinsonian Rats

Supplementary Methods

Expression of GFRα1 and GFRα2

Expression of GFRα1 and GFRα2 was tested by western blotting. MG87RET cells were transiently transfected with full-length human GFRα1 cDNA sub-cloned in pCDNA6 vector (Invitrogen, USA) or human GFRα2 cDNA in pCR3.1 using Lipofectamine 2000 (Invitrogen), as described by the manufacturer. The cells were starved for 4 h before the treatments in serum-free DMEM containing 15 mM HEPES, pH 7.2 for 5 h. The cells were lysed with Laemmli buffer, resolved with 10% sodium dodecyl sulfate–polyacrylamide gel electrophoresis (SDS-PAGE) and then transferred on nitrocellulose membrane as described in detail in the main text. The membranes were blocked and probed overnight at 4°C with human GFRα1 antibody (1:2000, R and D, Cat# AF714) and human GFRα2 antibody (1:2000, R and D, Cat# AF429). The membrane was washed and incubated with rabbit anti-goat horseradish peroxidase (HRP)-conjugated secondary antibody. After washing, the bands were visualized with ECL reagent (Pierce Biotechnology, USA) using Luminescent Image Analyzer LAS-3000 (Fujifilm, Japan).

Analysis of the phosphorylation pattern of RET's tyrosine residues

The pattern of tyrosine residue phosphorylation of RET was assessed by immunoprecipitation and western blotting performed in similar way as described in detail in the main text. The primary antibodies used for the experiment were as follows: anti-pY905Ret, anti-pY1015Ret, anti-pY1062Ret, and anti-pY1096Ret, diluted 1:3000 in blocking solution (a kind gift of Dr. Brian

Pierchala [1,2]). The membrane was washed and incubated with HRP-conjugated secondary anti-rabbit (GE Healthcare, Cat# NA9340V) antibody diluted 1:3000 in TBS-T with 3% skimmed milk for 1 h at room temperature. After washing, the bands were visualized with ECL reagent (Pierce Biotechnology) using Luminescent Image Analyzer LAS-3000 (Fujifilm). Equal loading of proteins in different wells was confirmed by re-probing the membrane with primary anti-RET C-20 antibody (1:500, Santa Cruz Biotechnology, Cat# sc-1290) and secondary anti-goat antibody (1:500, Agilent Dako, Cat# P0449).

Luciferase assay

To check the specificity of BT44 towards RET, we tested the activation of intracellular signaling via TrkB using reporter-gene based systems described in detail previously [3,4]. MG87 murine fibroblast cells were stably transfected with Pathdetect Elk-1 and TrkB. Cells were plated in 96-well plate at 200 000 cells/ml in DMEM, 10% FBS, 100 µg/ml Normocin (Invivogen, Cat# ant-nr-1), 1% DMSO, 15 mM Hepes pH 7.2. Next day, both BT44 and BDNF were applied in desirable concentration and incubated overnight. Cells were lysed and luciferase activity was measured using a luciferase detection reagent (LAR, Promega).

Assessment of TH-immunoreactive (TH-ir) neurites in the STR

TH-ir Neurites in the STR were counted by using an automated CNN algorithm and cloud-embedded Aiforia^{TM} platform. Briefly, TH-immunostained striatal sections were digitized using Pannoramic P250 Flash II whole slide scanner (3DHistech, Hungary) with extended focus. The digitized images were uploaded to Aiforia^{TM} image processing platform (Aiforia Technologies Oy, Finland). Number of TH-ir neurites in the dorsal striatum was measured bilaterally from 4 different

rostro-caudal levels through the striatum (approximately A/P +1.2, +0.48, and –0.26, mm relative to the bregma by an observer blind to the treatment groups. Subsequently, the number of TH-ir neurites within the demarcated areas was analyzed using the CNN algorithm that was trained to recognize TH-ir neurites from the digital images. The neurite density data (neurite number divided by /mm^2) are presented as percentage of the lesioned side as compared to the intact side.

CEREP screening

To evaluate potential safety-relevant off-target effects, 1 μM BT44 was screened in a panel of biochemical assays by CEREP company (Eurofins France 2019). Compound was tested for the ability to influence the following targets: adenosine receptors A1 (Cat# 0002) and A2B (Cat# 0005); adrenergic receptors alpha 1 (Cat# 0008), alpha 2 (Cat# 0011) and beta 3 (Cat# 3963); cannabinoid receptor CB1 (Cat# 0036); cholecystokinin receptors CK1 (Cat# 0039) and CCK2 (Cat# 0041); dopamine receptors D1 (Cat# 0044) and D2L (Cat# 1405); GABA receptor GABAB (Cat# 0885); histamine receptors H1 (Cat# 0870) and H2 (Cat# 1208); neurokinin receptor NK1 (Cat# 0100), NK2 (Cat# 0102) and NK3 (Cat# 0104); neurotensin receptor (Cat# 0465); opioid receptors delta (Cat# 0114, 2568), kappa (Cat# 1971) and mu (Cat# 0118); vasoactive intestinal peptide receptors (Cat# 1518); serotonin receptors 5HT1A (Cat# 0131), 5-HT1D (Cat# 1974), 5-HT2A (Cat# 0471) and 5-HT2C (Cat# 0137, 1003); Ca^{2+} ion channel (Cat# 0162); KATP channel (Cat# 0165); norepinephrine transporter (Cat# 0355); dopamine transporter (Cat# 0052); serotonin transporter (Cat# 0439); monoamine oxidase A (Cat# 0443); catechol-O-methyltransferase (Cat# 0457); protein serine/threonine phosphatase PP2A (Cat# 3953); protein tyrosine phosphatase PTPRC (Cat# 3956); TrkA (kinase activity *in vitro*, Cat# 2901), TrkB (kinase activity *in vitro,* Cat# 2902); TrkC (kinase activity *in vitro,* Cat# 3080); and RET (kinase activity *in vitro,* Cat#

1593). The standard CEREP company protocols were used for screening. All tests we run in duplicate. Results are presented as average of the two repeats.

REFERENCES

[1] Runeberg-Roos P, Virtanen H, Saarma M (2007) RET(MEN 2B) is active in the endoplasmic reticulum before reaching the cell surface. *Oncogene* **26**, 7909–7915.

[2] Tsui-Pierchala BA, Ahrens RC, Crowder RJ, Milbrandt J, Johnson EM (2002) The long and short isoforms of Ret function as independent signaling complexes. *J Biol Chem* **277**, 34618–34625.

[3] Sidorova YA, Bespalov MM, Wong AW, Kambur O, Jokinen V, Lilius TO, Suleymanova I, Karelson G, Rauhala PV, Karelson M, Osborne PB, Keast JR, Kalso EA, Saarma M (2017) A novel small molecule GDNF receptor RET agonist, BT13, promotes neurite growth from sensory neurons in vitro and attenuates experimental neuropathy in the rat. *Front Pharmacol* **8**, 365.

[4] Sidorova YA, Mätlik K, Paveliev M, Lindahl M, Piranen E, Milbrandt J, Arumäe U, Saarma M, Bespalov MM (2010) Persephin signaling through GFRalpha1: the potential for the treatment of Parkinson's disease. *Mol Cell Neurosci* **44**, 223–232.

Web references

Eurofins France 2019. http://www.cerep.fr/cerep/utilisateurs/index.asp, visited 15.12.2019

Eurofins Scientific 2019. https://www.eurofins.com/biopharma-services, visited 15.12.2019

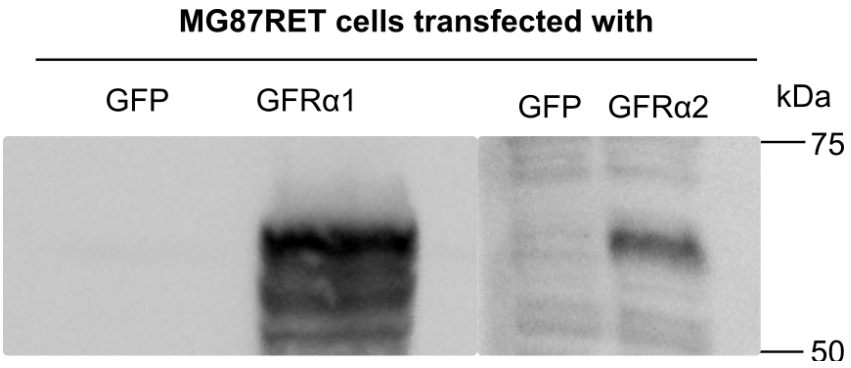

Supplementary Figure 1. Expression of GFRα1 and GFRα2 when transfected to MG87RET cells. GFP-transfected cells were used as negative control.

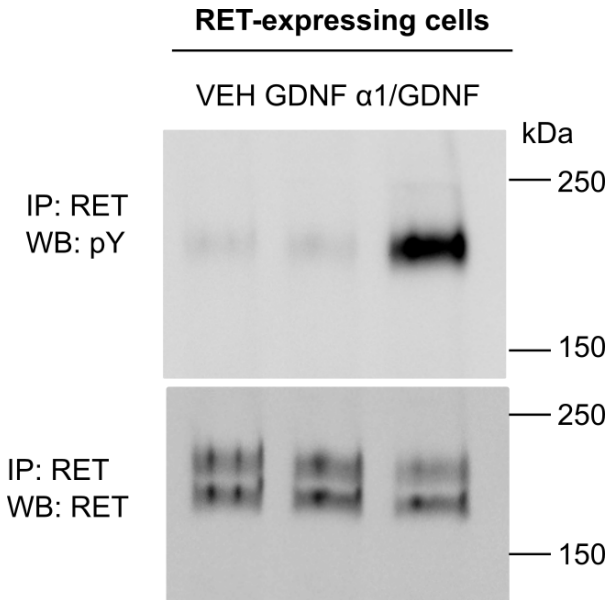

Supplementary Figure 2. GDNF does not induce RET phosphorylation in the absence of GFRα1. Soluble GFRα1-GDNF complex (represented as α1/GDNF) induces RET phosphorylation. Concentration of α1/GDNF: 200 ng/ml). VEH, vehicle; IP, immunoprecipitation; WB, western blotting.

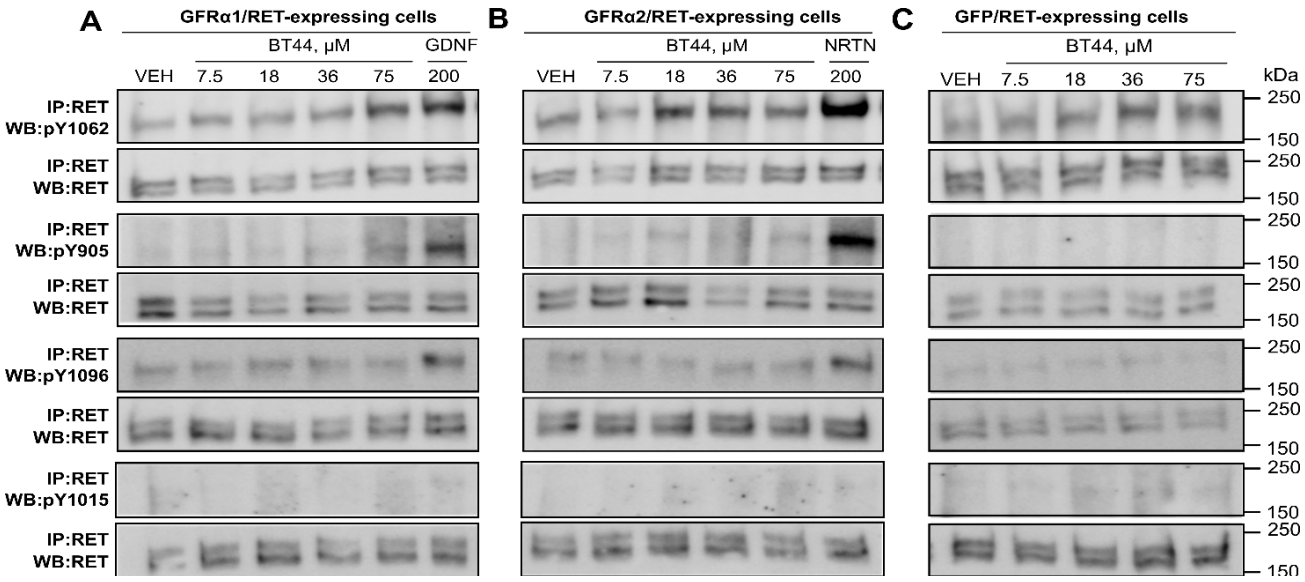

Supplementary Figure 3. BT44 induces autophosphorylation of various RET tyrosine residues in similar manner to GFLs. MG87RET cells transfected with co-receptor GFRα1 (A), GFRα2 (B), and GFP (C) were stimulated with different concentrations of BT44. GDNF and NRTN were used as positive controls for GFRα1 and GFRα2-transfected MG87RET cells, respectively. First, third, fifth, and seventh panels: western blot of MG87RET cells treated with vehicle (VEH), BT44 (7.5-75 μM), GDNF (200 ng/ml), or NRTN (200 ng/ml), probed with antibodies against pY1062, pY905, pY1096, and pY1015, respectively. Second, fourth, sixth, and eighth panels: the same membranes re-probed with anti-RET antibody. VEH, vehicle; IP, immunoprecipitation; WB, western blotting.

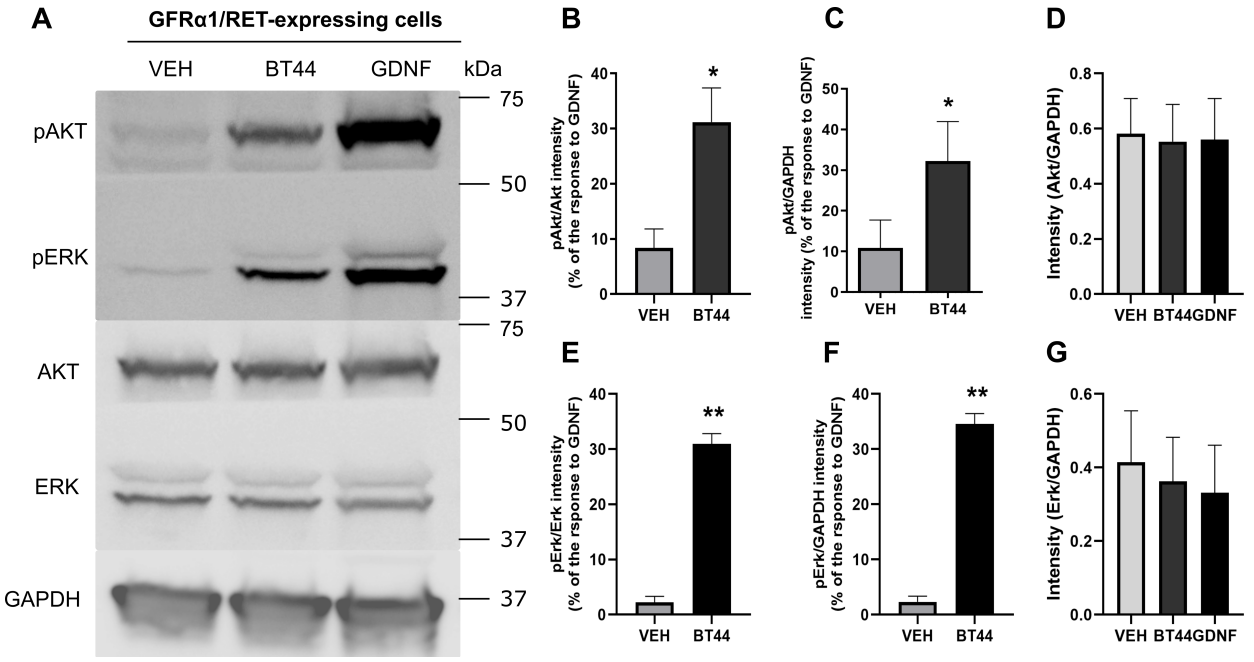

Supplementary Figure 4. BT44 and GDNF do not influence the protein level of either AKT or ERK. MG87RET cells transfected with co-receptor GFRα1 and stimulated with 75 μM BT44 or GDNF. A) Representative image of western blot with antibodies against AKT, pAKT, ERK, pERK and GAPDH. B, E) Quantification of pAKT and pERK levels relative to AKT and ERK, respectively. The data are presented as percentage of the protein phosphorylation in response to GDNF treatment. C, F) Quantification of pAKT and pERK levels relative to GAPDH. The data are presented as percentage of the protein phosphorylation in response to GDNF treatment. D, G) Quantification of total AKT and ERK protein levels relative to GAPDH. GDNF (200 ng/ml ≃ 6.6 nM) was used as a positive control. VEH, vehicle; GAPDH, glyceraldehyde 3-phosphate dehydrogenase. *$p < 0.05$, **$p < 0.01$, Paired t test (B, C, E, and F). RM ANOVA with Dunnett's *post hoc* test (D and G). Mean ± SEM, n = 3.

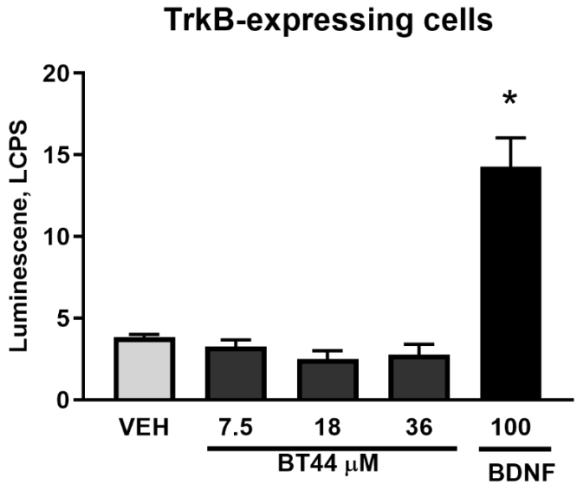

Supplementary Figure 5. BT44 does not elicit biological response in the absence of RET. BT44 failed to increase luciferase activity in reporter cells expressing TrkB. Cells were treated with BT44 (7.5-36 μM) or BDNF (100 ng/ml). Concentrations of BDNF is provided in ng/ml. VEH, vehicle. *$p < 0.05$, RM ANOVA with Dunnett's post hoc test. Mean ± SEM, Number of wells (n) = 4

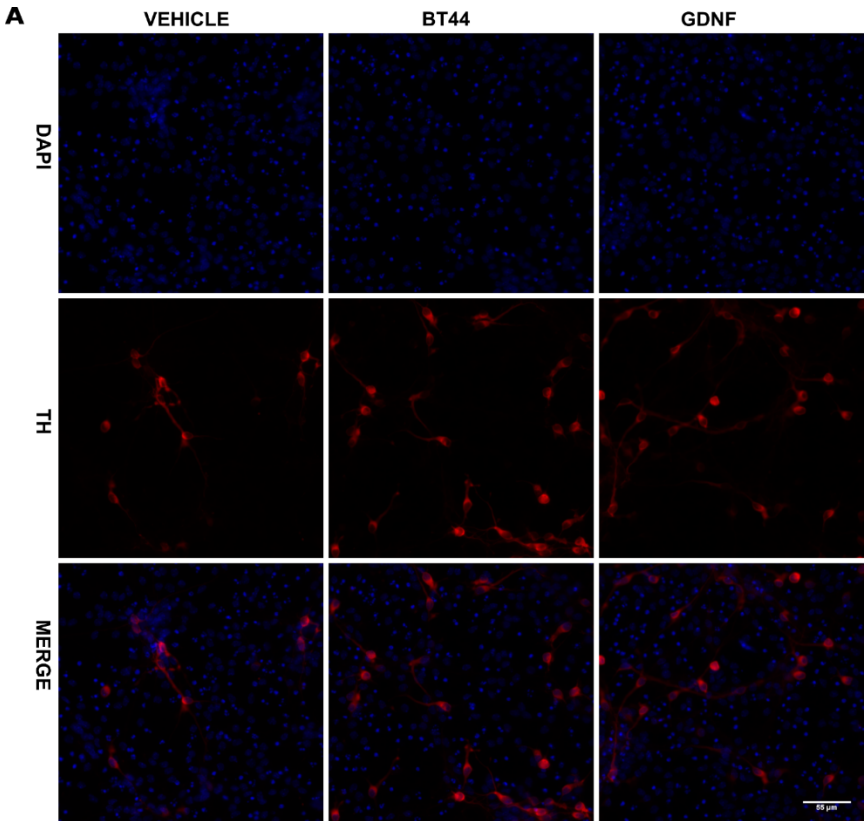

Supplementary Figure 6. Representative images of mouse embryonic E13.5 wild-type dopamine neuron cultures treated with vehicle, BT44, and GDNF, and probed with anti-TH antibody. Scale bar - 55 µm.

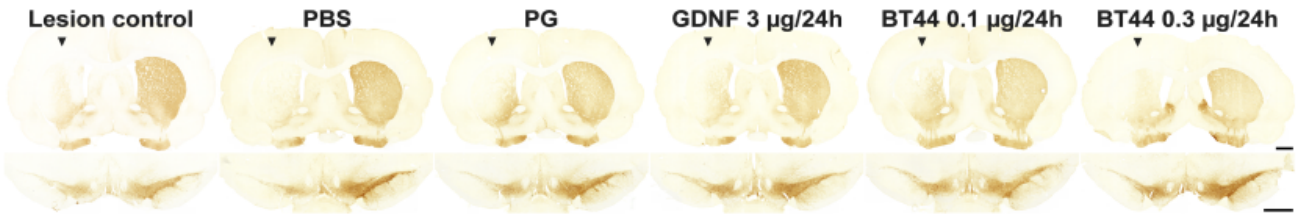

Supplementary Figure 7. Representative images of TH-immunostained coronal sections from the striatum (upper panel) and the ventral midbrain (lower panel) at 12 weeks post lesion. The lesion-side is denoted with an arrowhead. Scale bars - 1 mm.

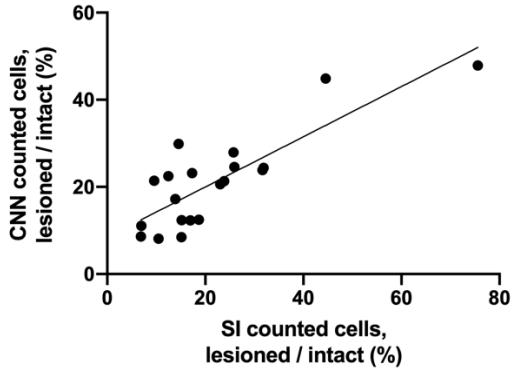

Pearson correlation coefficient (r):	0.8304
T statistic:	6.3235
Df:	18
p value:	5,8503E-06

Supplementary Figure 8. Correlation between stereological (Stereo Investigator®, SI) and convolutional neural networks (CNN) algorithm-based quantification of TH-ir cell bodies in the lesioned SNpc as compared to the intact side in a sub-cohort of 6-OHDA lesioned rats (total n = 20).

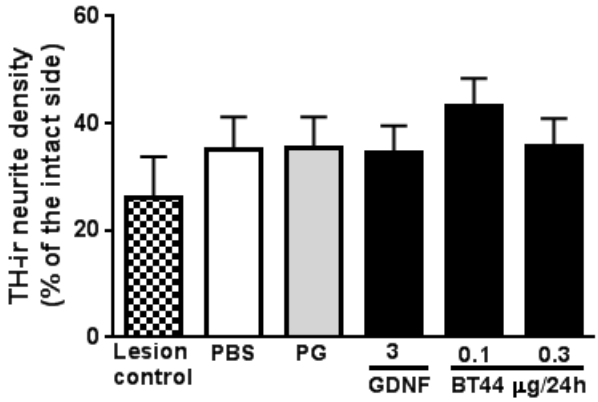

Supplementary Figure 9. **Effect of BT44 and GDNF on the TH-immunoreactive neurite number in the striatum in the in 6-OHDA lesioned rats.** Results are expressed as neurite numbers divided by /mm^2. Mean ± SEM, lesion control group n = 4, other groups n = 8-11

Supplementary Table 1. Comparison of TH-ir cell counts in the SNpc in a sub-cohort of 6-OHDA lesioned rats as quantified with automated convolutional neural networks (CNN) algorithm (Aiforia™) and stereological cell counting method (Stereo Investigator®).

		CNN			***Stereology***		
Treatment group	**n**	**Intact side**	**Lesioned side**	**Lesioned/Intact side (%)**	**Intact side**	**Lesioned side**	**Lesioned/Intact side (%)**
Lesion control	4	1329.0 ± 87.3	299.8 ± 33.5	22.8 ± 2.6	486.2 ± 54.3	60.5 ± 6.6	12.6 ± 1.1
PG	5	1392.6 ± 75.2	183.4 ± 39.4	13.3 ± 2.9	505.2 ± 41.9	83.5 ± 17.4	16.7 ± 3.1
GDNF 3 µg/24h	6	1335.5 ± 152.2	431.2 ± 112.1	30.5 ± 5.1	361.6 ± 55.8	130.2 ± 23.9	38.4 ± 8.1
BT44 0.3 µg/24h	5	1186.8 ± 58.3	193.2 ± 42.5	16.5 ± 3.8	395.3 ± 40.5	59.9 ± 13.6	15.1 ± 3.2

TH-ir cells in each brain were counted with CNN algorithm from 6 sections, and with stereological method from 3 sections (using the medial terminal nucleus of the accessory optic track as anatomical landmark). Data are expressed as total cell counts on the analyzed sections (CNN), or estimated cell population (Stereology); Mean ± SEM.

Supplementary Table 2. CEREP screening of 1 μM BT44.

Assay (assay type) [1]	Cat. No.	% inhibition from control	Reference Compound	IC_{50} Ref (M)	Ki Ref (M)
G protein-coupled receptors					
Adenosine receptors					
A1 (h) (antagonist radioligand)	0002	2.7	DPCPX	8.8E-10	5.6E-10
A2B (h) (antagonist radioligand)	0005	-14.7	NECA	5.8E-07	5.3E-07
Adrenergic receptors					
Alpha 1 (non-selective) (antagonist radioligand)	0008	-2.5	prazosin	4.3E-10	1.1E-10
Alpha 2 (non-selective) (antagonist radioligand)	0011	-4.6	yohimbine	8.6E-08	3.7E-08
Beta3 (non-selective) (antagonist radioligand)	3963	4.7	Alprenolol	1.7E-07	1.3E-07
Cannabinoid receptors					
CB1 (h) (agonist radioligand)	0036	19.4	CP 55940	1.4E-09	1.3E-09
Cholecystokinin receptors					
CCK1 (CCKA) (h) (agonist radioligand)	0039	5.7	CCK-8s	8.3E-11	6.2E-11
CCK2 (CCKB) (h) (agonist radioligand)	0041	9.7	CCK-8s	1.1E-10	4.3E-11
Dopamine receptors					
D1 (h) (antagonist radioligand)	0044	-11.4	SCH 23390	2.9E-10	1.1E-10
D2L (h) (antagonist radioligand)	1405	-4.4	butaclamol	1.9E-09	4.9E-10
GABA receptors					
GABAB(1b) (h) (antagonist radioligand)	0885	-8.9	CGP 54626	1.2E-09	5.9E-10
Histamine receptors					
H1 (h) (antagonist radioligand)	0870	5.6	pyrilamine	1.9E-09	1.2E-09
H2 (h) (antagonist radioligand)	1208	17.5	cimetidine	4.6E-07	4.5E-07
Muscarinic receptors					
M1 (h) (antagonist radioligand)	0091	0.8	pirenzepine	3.3E-08	2.9E-08
M2 (h) (antagonist radioligand)	0093	-5.1	methoctramine	3.3E-08	2.3E-08
M3 (h) (antagonist radioligand)	0095	10.9	4-DAMP	1.3E-09	9.4E-10
M4 (h) (antagonist radioligand)	0096	12.3	4-DAMP	9.0E-10	5.5E-10
Neurokinin receptors					

NK1 (h) (agonist radioligand)	0100	-12.2	[Sar9,Met(O2) 11]-SP	3.6E-10	1.6E-10
NK2 (h) (agonist radioligand)	0102	13.7	[Nleu10]-NKA (4-10)	2.2E-09	1.2E-09
NK3 (h) (antagonist radioligand)	0104	1.5	SB 222200	1.2E-08	6.5E-09
Neurotensin receptors					
NT (non-selective) (agonist radioligand)	0465	-1.6	neurotensin	2.9E-09	2.7E-09
Opioid receptors					
Delta (DOP) (h) (agonist radioligand)	0114	6.1	DPDPE	4.1E-09	2.4E-09
Kappa (KOP) (agonist radioligand)	1971	0.8	U 50488	1.2E-09	8.2E-10
Mu (MOP) (h) (agonist radioligand)	0118	5.6	DAMGO	4.1E-10	1.7E-10
PAC1 (PACAP) (h) (agonist radioligand)	1518	3.8	PACAP1-38	2.2E-10	1.9E-10
Serotonin receptors					
5-HT1A (h) (agonist radioligand)	0131	-2.1	8-OH-DPAT	1.1E-09	6.7E-10
5-HT1D (agonist radioligand)	1974	16.2	serotonin	4.4E-09	1.5E-09
5-HT2A (h) (agonist radioligand)	0471	9.2	(±)DOI	2.3E-10	1.7E-10
5-HT2C (h) (antagonist radioligand)	0137	5.6	RS 102221	3.0E-09	9.9E-10
5-HT2C (h) (agonist radioligand)	1003	11.7	(±)DOI	4.6E-10	4.2E-10
Ion channels and transporters					
Ca2+ channel (L, diltiazem site) (benzothiazepines) (antagonist radioligand)	0162	17	diltiazem	3.3E-08	2.6E-08
KATP channel (antagonist radioligand)	0165	4	glibenclamide	1.1E-10	3.7E-11
Norepinephrine transporter (h) (antagonist radioligand)	0355	15.2	protriptyline	6.4E-09	4.8E-09
Dopamine transporter (h) (antagonist radioligand)	0052	8.8	BTCP	1.2E-08	6.5E-09
5-HT transporter (h) (antagonist radioligand)	0439	-5.3	imipramine	3.2E-09	1.5E-09
Dopamine metabolism					
MAO-A (antagonist radioligand)	0443	11.3	clorgyline	1.3E-09	7.8E-10
COMT (catechol- O-methyl transferase)	0457	-1.9	Ro 41-0960	2.8E-08	
Phosphatases					
Protein Serine/Threonine Phosphatase, PP2A	3953	-10.4	calyculin A	4.9E-10	

Protein Tyrosine Phosphatase, PTPRC (CD45)	3956	-0.9	(NH4)6Mo7O24	9.9E-08
Kinases				
TrkA (h)		-4.1	staurosporine	1.2E-08
TrkB (h)		5.3	staurosporine	2.1E-09
TrkC (h)		-15.8	staurosporine	2.8E-09
RET kinase (h)		-11.6	staurosporine	2.8E-08

Supplementary Table 3. The number of TH-ir cells bodies in the SNpc on the intact and lesioned hemisphere as quantified with automated convolutional neural networks (CNN) algorithm.

Treatment group	n	Intact side	Lesioned side	Lesioned/Intact side (%)
Lesion control	4	1329.0 ± 87.3	299.8 ± 33.5	22.8 ± 2.6
PBS	9	1159.6 ± 74.1	132.1 ± 11.8	11.5 ± 0.9
PG	10	1323.8 ± 68.0	164.4 ± 11.8	12.6 ± 0.9
GDNF 3 µg/24h	11	1271.2 ± 89.4	382.9 ± 61.2	29.1 ± 2.8
BT44 0.1 µg/24h	10	1097.8 ± 55.6	180.5 ± 30.2	17.2 ± 3.3
BT44 0.3 µg/24h	10	1254.9 ± 47.6	192.0 ± 22.9	15.4 ± 1.9

Data are expressed as total cell counts on 6 sections (collected at six section intervals) encompassing the full rostro-caudal extent of the SNpc; Mean ± SEM.